Improved Renal Cortical SPECT of Neonates and Young Infants Using Narrow Imaging Pallets

Jeffrey A. Cooper and Brian K. McCandless

Departments of Radiology, Pediatrics and Medicine, Albany Medical Center, Albany, New York

Objective: The widths of most commercially-made imaging pallets limit the resolution of ^{99m}Tc DMSA SPECT imaging in neonates and young infants. We constructed a pediatric imaging pallet for ^{99m}Tc DMSA SPECT of neonates and young infants designed to allow close apposition of the camera to these patients during the entire orbit.

Methods: We designed the imaging pallet to replace the standard removable pallet on the imaging stand of a commercial gamma camera. The device consisted of two parts: a steel bracket attached to the imaging stand and a polyvinyl chloride imaging pallet. The imaging pallet consisted of interchangeable 15.24-cm (6-in) or 20.32-cm (8-in) diameter, 6.35-mm (1/4-in) thick polyvinyl chloride plumbing pipes cut in half lengthwise.

Results: The pallets were mechanically stable with loads 3 times that expected in clinical practice. Attenuation was acceptable and comparable to commercial pallets. The hemicylindrical shape provided side support and reduced patient motion, as well as allowing closer apposition of the camera head to the patient. The quality of these ^{99m}Tc DMSA SPECT images compared favorably with those obtainable in older children and adults. Specifically, the renal cortices were well delineated from the collecting systems and anatomic detail of normal cortex could be readily distinguished from abnormal cortex.

Conclusion: Custom pediatric imaging pallets optimized for use in neonates and small children can be constructed inexpensively. These pallets are easy to use and are stable. Use of these pallets can optimize ^{99m}Tc DMSA SPECT images of neonates and young infants.

Key Words: technetium-99m DMSA; SPECT; pediatric imaging

J Nucl Med Technol 1999; 27:127–131

The optimal management of the child with recurrent urinary tract infections or reflux requires periodic renal cortical scintigraphy with ^{99m}Tc DMSA (*1*). Renal cortical images can be acquired either with planar technique with a parallel-hole, converging or pinhole collimator or by SPECT (*2*). In general the diagnostic accuracy of ^{99m}Tc DMSA studies acquired with SPECT equals and may exceed that of studies acquired with planar technique (*3–5*). Many nuclear medicine physicians also find tomographic images easier to interpret and easier to present and explain to parents and referring physicians (*2,5*).

Optimal SPECT imaging requires that the camera be in close apposition to the patient for the entire acquisition orbit. With a parallel-hole collimator, image resolution decreases approximately linearly with increased distance from the patient. An increased distance between the camera and patient decreases the resolution of the projection images and degrades the resolution of the reconstructed tomographic images.

The widths of many commercial imaging pallets limit the resolution of ^{99m}Tc DMSA SPECT imaging in neonates and young infants. Most companies manufacture pallets with a width of 30.5–35.5 cm (12–14 in). In comparison, children less than 3 mo of age commonly have torso widths of 15 cm or less. The discrepancy between the widths of the standard imaging pallet and the average neonate's torso forces the camera to be 8–18 cm away from the patient during an orbit. This additional distance reduces resolution of the images and, thereby, greatly limits the utility of ^{99m}Tc DMSA SPECT in neonates and young infants. Imaging pallets designed for children can be purchased. However, manufacturers have optimized the width of these pallets for children over the age of 12 mo. Therefore, even commercial pediatric pallets fail to optimize the imaging of neonates and young infants, as they do not allow close opposition of the camera to these patients.

We constructed a pediatric imaging pallet for ^{99m}Tc DMSA SPECT imaging of neonates and young infants designed to allow close apposition of the camera head to these patients during the entire orbit. Use of this pallet provides ^{99m}Tc DMSA SPECT images of neonates and young infants with a resolution similar to that obtained in adults and older children.

MATERIALS AND METHODS

We designed the imaging pallet to replace the standard removable pallet on the imaging stand of a commercial gamma camera (Siemens Orbiter, Siemens Corp., Hoffman Estates, IL). The device consisted of 2 parts: a steel bracket attached to the

For correspondence or reprints contact: Jeffrey A. Cooper, MD, Nuclear Medicine, a-72, 47 New Scotland Ave., Albany Medical Center, Albany, NY 2208.

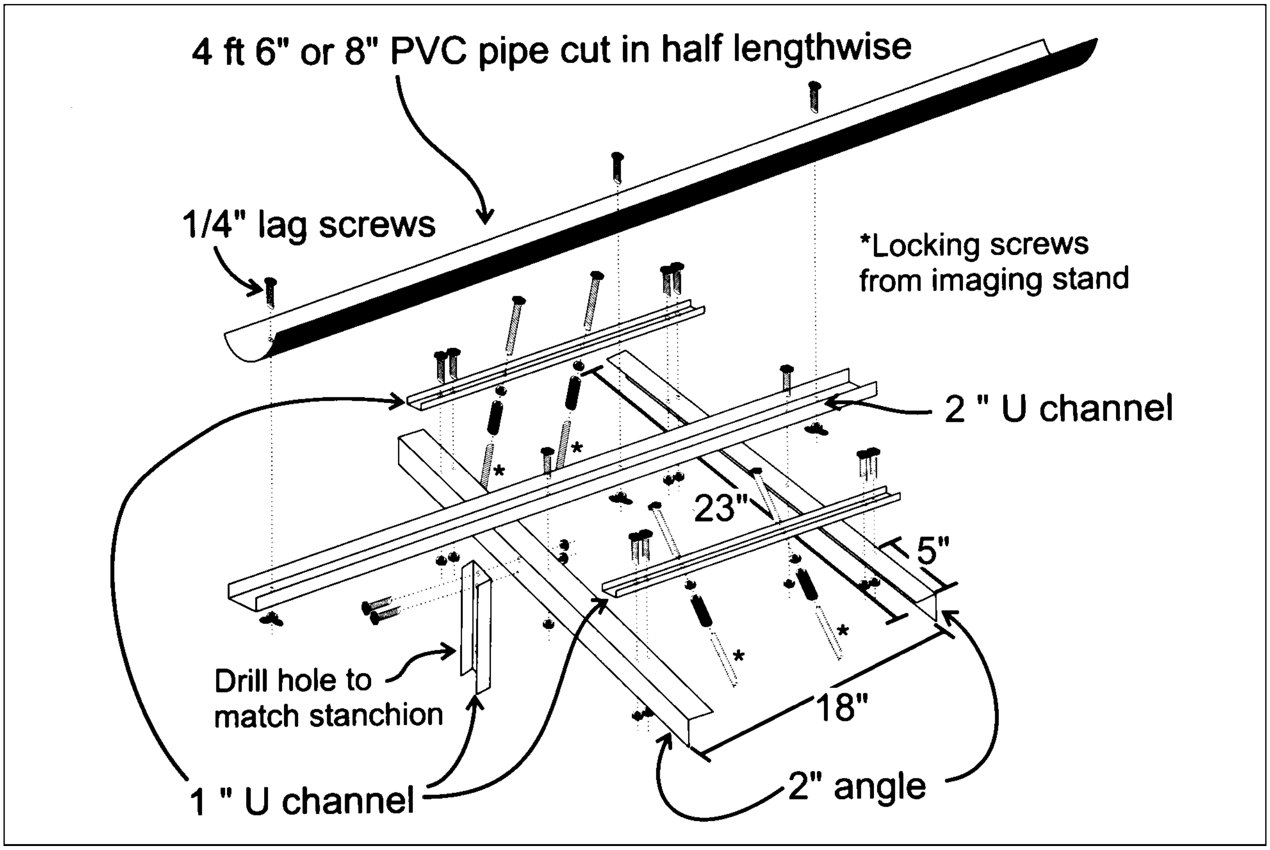

FIGURE 1. Construction details of the pediatric imaging pallet and support bracket.

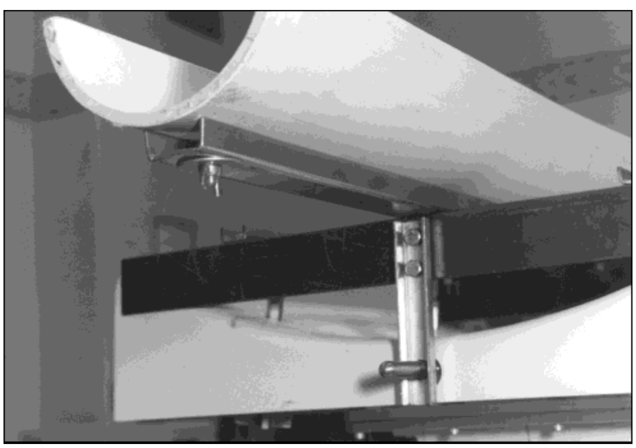

FIGURE 2. The bracket's vertical U-channel attaches to the imaging stand's stanchion pin and the PVC pipe attaches to the bracket.

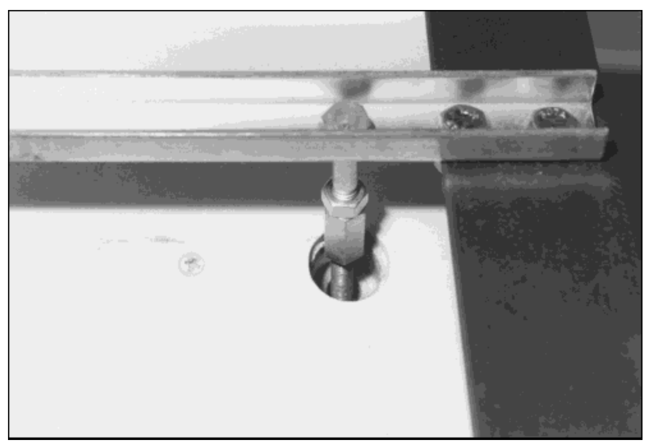

FIGURE 3. The imaging stand locking screws attach to the bracket using 1/4-in couplers.

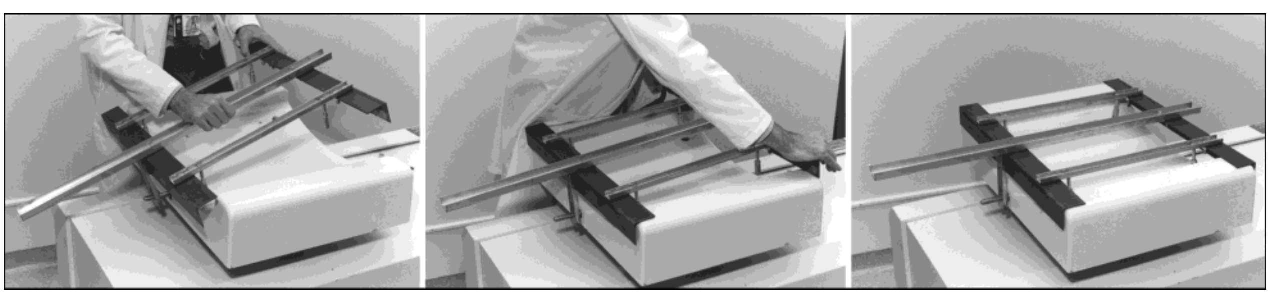

FIGURE 4. The attachment of the bracket to the imaging stand. Left, the bracket is angled so that the hole in the vertical U-channel aligns with and slides over the stanchion pin on the imaging stand. Middle, the bracket rests on the side of the imaging table opposite the stanchion pin and firm pressure slides it into place. Right, after attachment of the table locking screws, the bracket is in place and the correct size pallet can be attached with wing nuts.

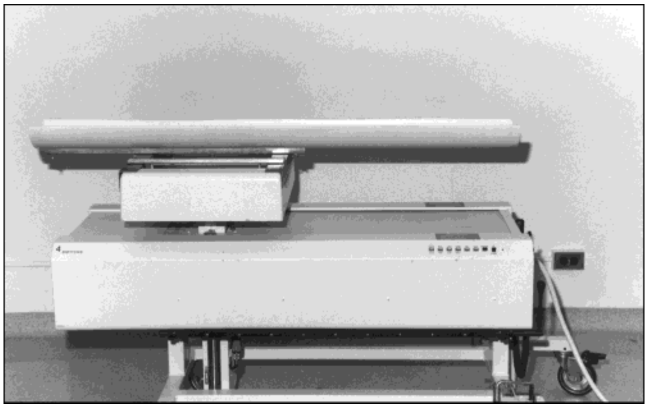

FIGURE 5. The assembled 15.24-cm (6-in) imaging pallet.

imaging stand and a polyvinyl chloride imaging pallet. The imaging pallet consisted of interchangeable 15.24-cm (6-in) or 20.32-cm (8-in) diameter, 6.35-mm (1/4-in) thick polyvinyl chloride plumbing pipes cut in half lengthwise. Construction details are shown in Figures 1, 2 and 3. We obtained the items for the steel bracket from a hardware store for a cost of less than $100. Retail hardware and building supply outlets tend not to carry 15.24-cm or 20.32-cm diameter polyvinyl chloride pipe. We obtained the 15.24-cm and 20.32-cm diameter polyvinyl chloride pipe as a donation from the scrap of a commercial plumbing supply house. Otherwise, one can expect to pay up to $300 for this length and diameter of pipe.

The attachment of the bracket to the imaging stand is shown in Figure 4. Completed assemblies with the 15.24-cm (6-in) and 20.32-cm (8-in) wide imaging pallets bolted to the bracket are shown in Figures 5 and 6. The two imaging pallet sizes are interchangeable, allowing selection of a pallet width optimal for each patient. The imaging pallets can be preattached to the imaging bracket and attached to the imaging stand as one piece. The attachment of the bracket and pallet to the imaging stand allows full control of the position of the pallet position as with a standard adult pallet. We tested the stability of the device by placing weights on the ends of the pallets opposite the cantilever point.

Images were acquired 3 h after the intravenous injection of 75 µCi/kg ^{99m}Tc DMSA. In children without a suspicion of

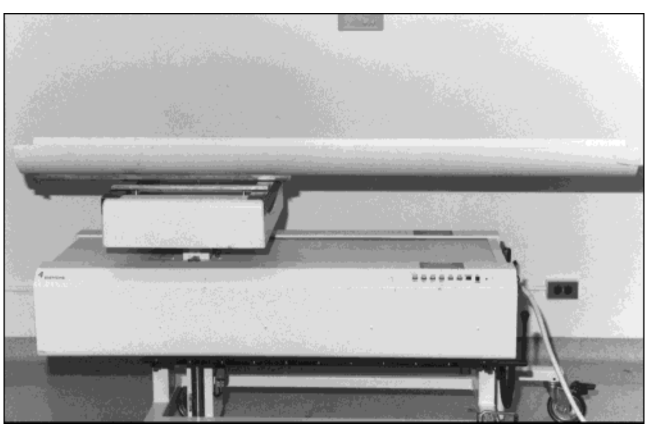

FIGURE 6. The assembled 20.32-cm (8-in) imaging pallet.

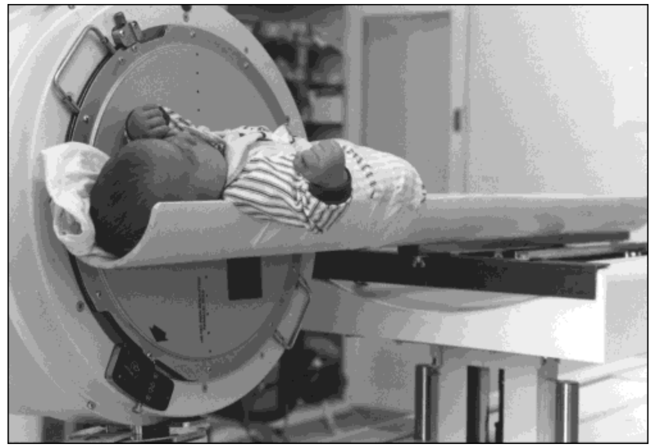

FIGURE 7. Four-week-old infant having ^{99m}Tc DMSA SPECT imaging while in a 15.24-cm (6-in) wide narrow imaging pallet.

ectopic kidneys, we obtained 64 images (128 × 128) over 180° for 15 s per image. Images were reconstructed with an order 10 Butterworth filter having a 0.4 Nyquist cutoff.

RESULTS

The 15.24-cm (6-in) wide pallet supported 23 kg-m of torque on the cantilever point with less than 1 cm of vertical displacement and less than 1 cm of rotational displacement. The 20.32-cm (8-in) wide pallet supported 36 kg-m of torque on the cantilever point with less than 1 cm of vertical displacement and less than 1 cm of rotational displacement. In comparison, a 10-kg child in the 15.24-cm wide pallet placed with a center of gravity at 30 cm from the cantilever point would be expected to exert 3 kg-m of torque on the cantilever point. A 20-kg child in the 20.32-cm wide pallet placed with a center of gravity at 50 cm from the cantilever point would be expected to exert 10 kg-m of torque on the cantilever point.

Figure 7 shows a neonate having ^{99m}Tc DMSA SPECT imaging. The technologists found the device acceptable and convenient. The camera was able to rotate within 1 cm of the patient during the entire orbit. The technologists noted that children seemed more comfortable, quiet and easy to position on the hemicylindrical surface than on a flat surface, due to lateral support and an apparent wrapping effect of the device. This advantage has led the technologists to use the narrow imaging pallets for planar studies, such as renal scans and bone scans.

Figures 8, 9 and 10 show the results of ^{99m}Tc DMSA SPECT scans of neonates and young infants imaged with the pediatric pallets. The quality of these ^{99m}Tc DMSA SPECT images compares favorably with those obtainable in older children and adults. Specifically, the renal cortices are well delineated from the collecting systems and anatomic detail of normal cortex can be distinguished readily from abnormal cortex.

DISCUSSION

Renal cortical imaging with ^{99m}Tc DMSA is indicated for detecting renal scarring and pyelonephritis, measuring differential function, and evaluating solitary, ectopic or dysmorphic

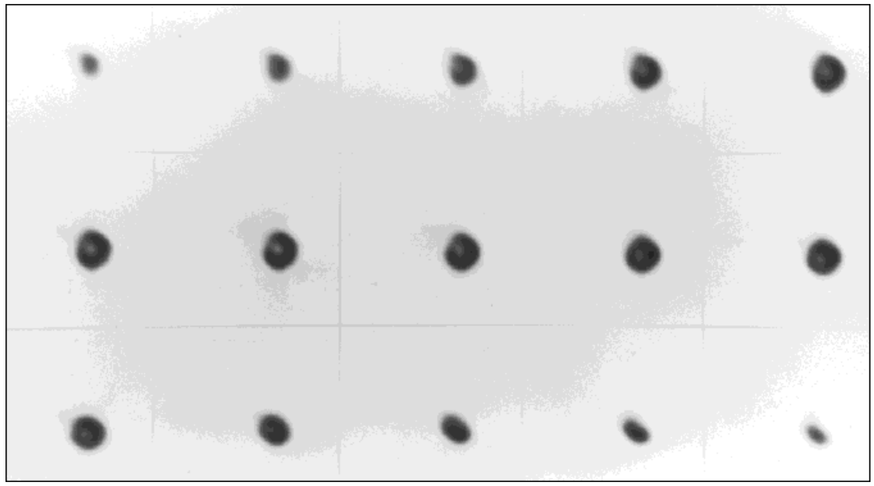

FIGURE 8. Transaxial images from a ^{99m}Tc DMSA SPECT performed on a 4-wk-old infant. The child was being evaluated for a right cystic kidney. The images show clear delineation of the left cortex from the collecting system.

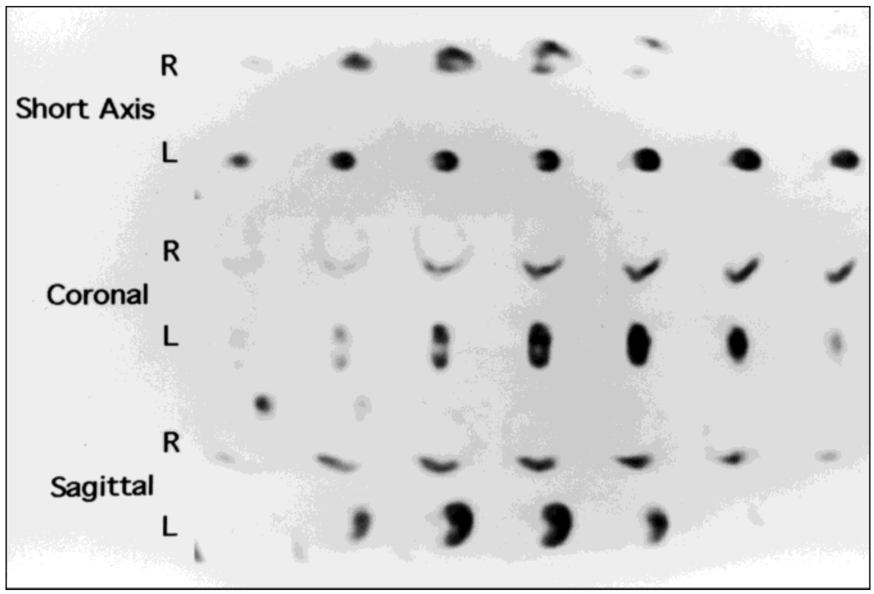

FIGURE 9. Short-axis, near coronal long-axis oblique and near sagittal long-axis oblique images of a 3-wk-old infant with a cystic right kidney. The left kidney (L) is normal and the cortex is delineated from the collecting system. The right kidney (R) demonstrates a markedly enlarged collecting system, normal cortex in the extreme lower pole and thinned, but not absent, cortex through the remainder of the kidney.

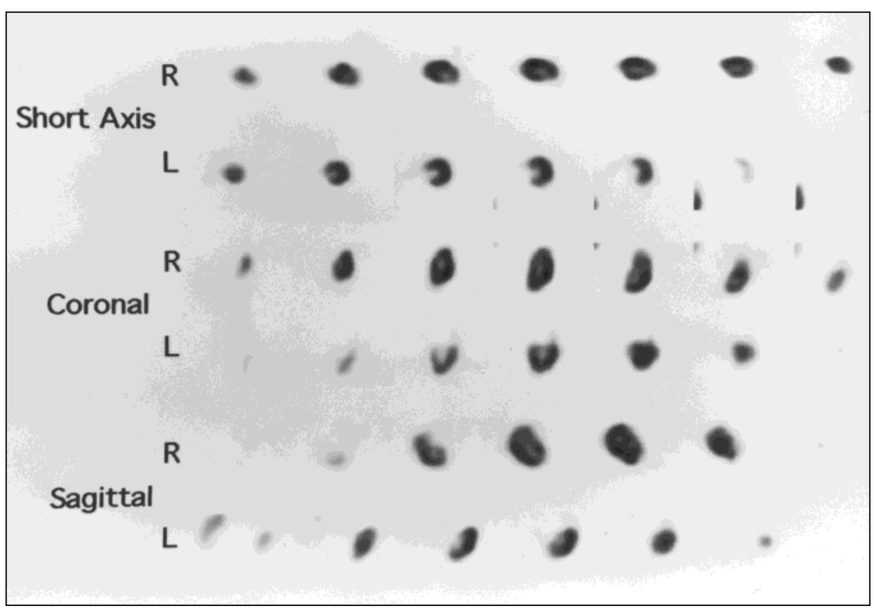

FIGURE 10. Short-axis, near coronal long-axis oblique and near sagittal long-axis oblique images of a 3-mo-old infant with a left duplication. The right kidney (R) is normal and the cortex is delineated from the collecting system. The left kidney (L) demonstrates a nonfunctioning upper pole cortex. The lower cortex is normal. The lower pole cortex is well delineated from the collecting system.

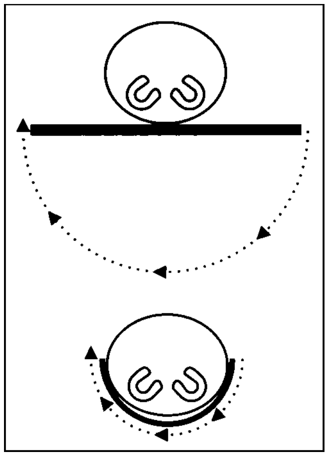

FIGURE 11. Comparison of a circular camera orbit around a child with a 15.24-cm (6-in) diameter torso on (top) a 30.5-cm (12-in) wide flat imaging pallet and (bottom) a 15.24-cm (6-in) hemicylindrical pallet. With a 180° circular orbit, the camera is always between 8 and 18 cm away from the patient on the flat pallet, but remains in close apposition to the patient on the hemicylindrical pallet.

kidneys (*2*). In managing urinary tract infections, renal cortical scintigraphy detects a common complication, has the highest level of accuracy, assesses the outcome of management and provides risk stratification (*2–4*). Currently, many urologists believe that renal cortical scintigraphy is an important imaging tool for the routine management of urinary tract infection (*1*).

Neonates have immature renal function and reduced glomerular filtration rate compared with older children and adults. This finding has led some authors to believe that neonates cannot be successfully imaged with ^{99m}Tc DMSA (*6*). However, the kidneys of neonates and older children show similar quantitative ^{99m}Tc DMSA uptake (*7*). Our experience supports the view that with a narrow imaging pallet and proper technique, high-quality renal cortical images can be obtained in neonates.

Optimal SPECT imaging requires that the camera be in close apposition to the patient for the entire acquisition orbit. With a parallel-hole collimator, image resolution decreases linearly with distance from the object. With a flat pallet and a 180° circular orbit, the camera will always be 8–18 cm away from a patient with a 15-cm torso width on a 30.5-cm (12-in) wide imaging pallet (Fig. 11). With a narrow hemicylindrical pallet and a 180° circular orbit, the camera can be in close apposition to the patient. This reduction of distance improves the resolution of the ^{99m}Tc DMSA SPECT images in neonates and young infants.

Unlike commercial solutions, our design serves the needs of neonates and young infants. In addition, our design is inexpensive, yet is stable and safe. Although our solution is designed for a specific make and model of gamma camera, the basic principle of mounting a narrow hemicylindrical imaging table to an imaging stand can be applied to other makes and models of gamma cameras.

Our imaging pallet may find use in other SPECT imaging studies, such as bone SPECT, brain SPECT and ^{123}I-MIBG SPECT, where standard adult or pediatric imaging pallets limit how close a gamma camera can get to the patient. In addition, our technologists have found the device useful for keeping children comfortable, quiet and positioned during planar imaging.

CONCLUSION

Optimal SPECT imaging requires that the camera be in close apposition to the patient for the entire acquisition orbit. The widths of many commercial imaging pallets limit the resolution of SPECT imaging in small children because the imaging pallet prevents the camera from remaining close to the patient during the camera orbit. We designed a set of interchangeable pediatric imaging pallets that allows close apposition of the camera to small children during the entire orbit. The shape provides lateral support for the patient and eases positioning. These pallets are inexpensive, easy to use and stable. They allow for ^{99m}Tc DMSA SPECT images of neonates and young infants with a resolution similar to that obtained in adults and older children.

REFERENCES

1. Rushton HG, Majd M, Jantausch B, Wiedermann BL, Belman AB. Renal scarring following reflux and nonreflux pyelonephritis in children: evaluation with ^{99m}technetium-dimercaptosuccinic acid scintigraphy. *J Urol.* 1992; 147:1327–1332.
2. Cooper JA. Kidney infection in children: role of nuclear medicine. In: Freeman LM, ed. *Nuclear Medicine Annual 1998*. Philadelphia, PA: Lippincott-Raven; 1998:225–246.
3. Majd M, Rushton HG, Chandra R, et al. Technetium-99m-DMSA renal cortical scintigraphy to detect experimental acute pyelonephritis in piglets: comparison of planar (pinhole) and SPECT imaging. *J Nucl Med.* 1996; 37:1731–1734.
4. Cook GJ, Lewis MK, Clarke SE. An evaluation of ^{99m}Tc-DMSA SPET with three-dimensional reconstruction in 68 patients with varied renal pathology. *Nucl Med Commun.* 1995; 16:958–967.
5. Everaert H, Flamen P, Franken PR, et al. ^{99m}Tc-DMSA renal scintigraphy for acute pyelonephritis in adults: planar and/or SPET imaging. *Nucl Med Commun.* 1996; 17:884–889.
6. Haycock GB. Development of glomerular filtration and tubular sodium reabsorption in the human fetus and newborn. *British J Urology*. 1998; 81(suppl):2:33–238.
7. Gorenberg M, Issaq E, Wald M, Groshar D. Quantitative SPECT uptake of technetium-99m-DMSA by the kidneys in children [Abstract]. *J Nucl Med.* 1998; 39:28P.